

**Biophysical Journal, Volume 122**

**Supplemental information**

**Different membrane order measurement techniques are not mutually consistent**

**Ankur Gupta, Mamata Kallianpur, Debsankar Saha Roy, Oskar Engberg, Hirak Chakrabarty, Daniel Huster, and Sudipta Maiti**

# Supplementary Information

## Different Membrane Order Measurement Techniques are Not Mutually Consistent

Ankur Gupta#, Mamata Kallianpur#, Debsankar Saha Roy#, Oskar Engberg\$, Hirak Chakrabarty^, Daniel Huster\$#\*, and Sudipta Maiti#\*

### 1. Materials and Methods

The lipids POPC (16:0-18:1 PC), POPG (16:0-18:1 PG), DOPC (18:1 ( $\Delta^9$ -Cis) PC), Egg-sphingomyelin, 1,2-dioleoyl-*sn*-glycero-3-phosphoethanolamine-N (lissamine rhodamine B sulfonyl) (18:1 Liss Rhod PE), Lipid extruding kit, 10 mm Filter Supports, Nucleopore Track-etched polycarbonate membrane (pore diameter 50 nm) were purchased from Avanti Polar Lipids Inc. (Alabaster, USA). Cholesterol and methyl- $\beta$ -cyclodextrin (m $\beta$ CD) were purchased from Sigma Aldrich (St. Louis, MO). Serotonin-hydrochloride was purchased from Merck (Darmstadt, Germany). Sodium chloride and calcium chloride dehydrate were purchased from Merck Life Science Private Limited (India). Chloroform and methanol AR graded were purchased from S. D. Fine Chemical Ltd. (India). All the chemicals were used without any additional purification. Supported bilayers were formed on mica (grade V4 muscovite) as support purchased from SPI supplies (West Chester, USA). All the experiments were performed using milli-Q water (conductivity 18.2 M $\Omega$  cm<sup>-1</sup>) obtained from a Milli-Q gradient system (Millipore, Germany).

#### 1.1. Preparation of supported bilayers

The mica supported lipid bilayer (SLB) was prepared by following the vesicle fusion method.<sup>1</sup> Two monophasic bilayers - pure POPG and POPC/POPG/cholesterol in the molar ratio of 1/1/1 (PPC111) were prepared by weighing the powders in the respective molar ratio and dissolving them in the chloroform solvent. To prepare a biphasic phase-separated bilayer, lipids DOPC/Egg SM/cholesterol in the molar ratio of 2/2/1/ (DEC221) were weighed and dissolved in the 1/1 (by volume) chloroform/methanol solvents. The solvent was then evaporated by purging with argon gas to make a dried film called lipid film. The dried lipid film was kept in a vacuum desiccator for ~24 hours to completely remove organic solvents which were then rehydrated using either milli-Q water or buffer (150 mM NaCl) to make a lipid suspension of concentration 2.5 mg/mL. The solution was vortexed properly for ~10 minutes to form multilamellar vesicles (MLVs). The MLVs were passed through an extruder (Avanti Polar Lipids Inc., Alabaster) containing a polycarbonate membrane of 50 nm pore size (covered by two 10 mm filter supports on each side of the membrane) using 1000  $\mu$ L vacuum-sealed syringes (Hamilton, Avanti Polar lipids Inc.) to obtain a clear solution containing uniform small unilamellar vesicles (SUVs). The extrusion was performed at 60°C. Bilayer was formed by adding 40  $\mu$ L of 100 mM calcium chloride solution, 50  $\mu$ L of SUVs, and 210  $\mu$ L of water (or buffer) together (all were preheated to 65°C in a water bath) on a freshly cleaved mica glued to a glass petri dish and keeping it in a water bath at 70°C for 1 hour. The vesicles fuse to form a bilayer in this condition. The excess unfused vesicles were removed by thoroughly rinsing the bilayer with water or buffer. The formation of lipid

bilayer was confirmed by the AFM force indentation study. The buffer composition is 145 mM NaCl, 5.4 mM KCl, 20 mM Na-HEPES, and pH 7.4.

## 1.2. AFM Force Indentation

All AFM measurements were recorded using the commercial NanoWizard II system (JPK Instruments, Berlin, Germany). The AFM instrument was mounted on an Axiovert Inverted Microscope (Zeiss, Germany). The calibration of sensitivity, resonance frequencies (both in air and in water), and determination of the spring constant was done before each force experiment using the thermal noise method.<sup>2</sup> The cantilever used for all the force experiments has a resonance frequency of 10-20 kHz and a spring constant of 0.03 N/m. Sensitivity and spring constant measurements were also performed after the end of each experiment. The sensitivity values were similar before and after the experiments within errors. All the AFM force experiments were performed on the supported bilayers which were formed on mica glued to coverslip glass in a liquid cell. The bilayer remained hydrated until the end of the experiment.

For all the bilayer force experiments, the total Z piezo displacement was 1.0  $\mu\text{m}$ . The piezo velocity both for approach and retraction was kept at 0.5  $\mu\text{m}\cdot\text{s}^{-1}$ . In the AFM force indentation study, a sharp AFM tip is brought to the SLBs from the top. The force remained zero when the tip is away from the top surface of the bilayer in the non-contact region (Figure 1A, a to b part of curve). As soon as the AFM tip hit the surface of the bilayer at the contact point, the force starts increasing. The tip continues to approach and indent into the membrane with increasing force (Figure 1A, b to c part of curve) till the membrane ruptures locally. This rupturing of the membrane is characterized by a 'kink' in the force vs tip z-displacement curve (Figure 1A, point c on the curve). After that, the tip approaches the hard mica surface and the force continues to increase till it reaches the force value set by us (Figure 1A, d to e part of curve). The force value corresponding to this 'kink' is known as the breakthrough force ( $F_x$ ) or the indentation force and it is the measure of the stiffness of the membrane. In general, stiffness is assumed to be proportional to the order of the membrane. So, the higher the stiffness of the membrane, the more ordered is the membrane. All the force experiments were carried out at different points on the bilayer. For each set, usually, 400-600 force curves were recorded. The force indentation curves were processed and analyzed using JPK Data Processing software. The breakthrough force values were extracted from each approach curve to build the histogram. The serotonin is incubated for 45 minutes for all the AFM experiments.

## 1.3. Spectral imaging of Nile red dye

The fluorescence spectra of supported bilayer bound Nile Red dye were obtained by performing confocal imaging in the lambda stacking mode on the commercial LSM 880. For lambda-stacking imaging, 514 nm excitation light was taken from an Ar++ laser, reflected by a dichroic mirror (MBS 514) and focused through a Zeiss C-Apochromat 40x, NA 1.2, water immersion objective onto the sample. The fluorescence emission was collected by the same objective and sent to the GaAsP detector through the monochromator with a resolution of 5 nm. Lambda stacks were independently acquired from 529 to 714 nm at the interval of 5 nm using an LSM 880 microscope (Carl Zeiss, Jena, Germany) with Zen imaging software. All the lambda imaging was done on the supported bilayers which were formed on the freshly cleaved mica already glued to coverslip glass in a Petri dish. Nile Red was incubated to SLBs with a concentration of  $\sim 1 \mu\text{M}$  for 20 minutes and the bilayer is washed to remove unbound Nile red as much as possible. The stock of Nile red was made in pure methanol and stored at

4°C for further use. The serotonin is incubated for 45 minutes for all the experiments. The nature and peak of the fluorescence spectra of Nile red are sensitive to the packing of the lipids. If we compare the fluorescence spectra of dye in the aqueous environment (Figure 1C, orange cartoon spectra), disordered membrane environment (Figure 1C, green cartoon spectra) and ordered membrane environment (Figure 1C, blue cartoon spectra), the spectra have relatively more contribution of lower wavelength in the ordered membrane environment compared to disordered membrane environment.

#### 1.4. Spectral Imaging of Laurdan

The multiphoton excitation of Laurdan is carried out on a modified confocal microscope (LSM 710, Carl Zeiss), which we have adapted for multiphoton excitation. Additionally, to enable us to use specific UV sensitive photomultiplier tubes (Electron Tubes, model: P30A-01, Electron Tubes Limited, UK) in the non-descanned path, we got two external additional signal input channels custom-made by the manufacturer. A Ti: sapphire laser (MaiTai DeepSee, Spectra-Physics) operating at 780 nm wavelength and producing ~100 fs pulses (repetition rate = 80 MHz) is used for multi-photon excitation of Laurdan, with the DeepSee chirp compensator adjusted for maximum signal. Our custom-built multi-photon microscopy setup uses relatively low laser powers (27–30 mW at the back aperture). The fluorescence signal is collected in the epifluorescence mode. The emission is sent to the non-descanned channel after the backscattered excitation light is separated from the Laurdan fluorescence by a dichroic mirror (690+, part of LSM 710, Carl Zeiss) in the fluorescence turret. The Laurdan fluorescence in the ordered membrane environment is bluer shifted in wavelength compared to the disordered membrane environment as shown in Figure 1K. The Laurdan fluorescence spectrum has a peak centred at ~ 425 nm for the ordered membrane environment and ~500 nm for the disordered membrane environment. So, a 50/50 dichroic beam-splitter is used to split the fluorescence signal of Laurdan into two channels- the blue channel and the green channel. The blue channel fluorescence was collected through the filter 425/30 (bandwidth of 410-440 nm) and green channel fluorescence was collected through the filter 500/30 (bandwidth of 485-515 nm). These signals are detected by two analog photomultiplier tubes (PMTs, model: P30A-01, Electron Tubes Limited, UK). All the settings such as detector gain, laser power, etc. kept the same during the experiment. All the multiphoton imaging was done on the SLBs which were formed on the freshly cleaved mica already glued to coverslip glass in a Petri dish. Laurdan was incubated to SLBs with a concentration of ~ 10 μM for 40 minutes and the bilayer is washed to remove unbound Laurdan as much as possible. The 1 mM stock of Laurdan was made in pure DMSO and stored at 4°C for further use. To quantify the order of the membrane by Laurdan dye, the Generalized Polarization (GP) of the membrane is calculated using equation 1. The complete flowchart to calculate the GP value from the obtained blue and green channel images is shown in Figure 1 (E to L). The representative membrane system in the flowchart is the phase-separated DEC221 SLB. This SLB has coexisting ordered and disordered phases at room temperature. The green channel (485-515 nm) and blue channel (410-440 nm) images are shown in Figures 1E and 1I respectively. The intensity image of both channels is computed in the ImageJ software and both the images are added (Figure 1F) and subtracted (Figure 1J) performing image arithmetic in ImageJ according to equation 1 to get the final GP image (Figure 1G). Then the average GP value is calculated from the GP image. The GP value for the monophasic bilayer such as the PPC111 bilayer is calculated simply by calculating the average GP of the whole image. But for phase-separated bilayers such as DEC221, GP for specific phases is calculated by selecting ROI separately for each phase and taking the average GP of the ROI.

$$GP = \frac{\text{Intensity of blue channel} - (G * \text{Intensity of green channel})}{\text{Intensity of blue channel} + (G * \text{Intensity of green channel})} \quad (1)$$

The G-factor is calculated by taking fluorescence measurement of Laurdan dye in pure DMSO in a commercial spectrofluorimeter Fluorolog 3 (Horiba, Jobin Yvon). The excitation wavelength was set to 385 nm and emission was collected from the 400-600 nm range. The fluorescence emission was separated into blue (average intensity from 410-440 nm) and green (average intensity from 485-515 nm) channels and the GP value was calculated from equation 1 by keeping  $G = 1$ . The obtained GP value was used to calculate G-factor. The same Laurdan dye in pure DMSO solution is used in the multiphoton imaging setup and intensity of blue and green channels are obtained. Now, the obtained GP value from the spectrofluorimeter and intensity of both channels in the multiphoton setup is put in equation 1 to obtain the G-factor. This G-factor was used to calculate the GP value of Laurdan in the supported bilayers. This calibration was done before each experiment.

### **1.5. Z-scan Fluorescence Correlation Spectroscopy (z-FCS) measurements**

Z-scan FCS measurements were done on a home built combined AFM-confocal setup as described in.<sup>3</sup> Briefly, the expanded pulsed 543 nm laser from a supercontinuum laser source was guided by the help of reflecting and dichroic mirrors and focused into the sample using an apochromatic 60× water immersion objective with the numerical aperture of 1.2 (Olympus, PA, USA). The objective was mounted in a microscope (Axiovert 100M, Germany). The fluorescence signal obtained from the sample was collected from the same objective and was passed through the filters and focused onto a 25 μm core diameter optical fibre using a 160 mm positive lens (tube lens) mounted in the microscope. This optical fibre acts as a confocal pinhole to eliminate the out-of-focus fluorescence photons. The fluorescence photons were detected by a single-photon avalanche photodiode (APD, PerkinElmer Inc., Waltham, MA, USA). The APD signal was read by a hardware correlator present in the PicoHarp300 module. The time traces of fluorescence intensity as a function of time were recorded using a correlator and Symphotime 32 software is used to calculate the raw autocorrelation function. The autocorrelation curves were recorded at different z-interval (along the bilayer axis) and at various xy coordinates in the sample by using an automated sample scanner (TAO-piezo scanner, Nanowizard II, JPK Instruments AG, Germany). The sample scanner was kept at a particular xy point and autocorrelation curves were recorded at different z-intervals by moving the scanner along the z-axis.

To perform the z-FCS measurements in the supported bilayers, the 18:1 Liss Rh PE was added with 0.05 mol% to the lipid mixture of the given molar ratio during lipid film preparation. All z-FCS experiments were done on the supported bilayers. The 5 mM serotonin is incubated for 45 minutes and the same points in the membrane are measured after serotonin addition.

The raw autocorrelation curves at each z were fitted with equation (2) in Origin 7.5 software (OriginLab, Northampton, MA, USA) to measure characteristic diffusion times  $\tau_{D1}$  and  $\tau_{D2}$  for the two components, amplitudes  $g_1$  and  $g_2$  of both diffusing components, triplet state fraction  $f$  and triplet state lifetime  $\tau_1$  of the dye and the background level  $bl$ . The autocorrelation curve is fitted with two diffusion components as there could be traces of unfused free vesicles in the bulk solution. The longer diffusion time is considered for further analysis as it is coming due to the diffusion of lipids in the supported bilayer. The diffusion

times at all z-interval were fitted with equation (5) to obtain the diffusion coefficient  $D_T$  value of lipids in the supported lipid bilayers.

$$(2) G(\tau) = \left( \frac{1-f+f*e^{-\frac{t}{\tau_1}}}{1-f} \right) * \sum_{i=1}^2 \left[ \frac{g_i}{1+\frac{t}{\tau_{Di}}} \right] + bl$$

$$(3) \tau_D = \left( \frac{w^2}{4*D} \right)$$

$$(4) w^2 = \left( w_0^2 \right) \left( 1 + \frac{\lambda^2(\Delta z)^2}{\pi^2 n^2 w_0^4} \right)$$

$$(5) \tau_D = \left( \frac{w_0^2}{4*D} \right) \left( 1 + \frac{\lambda^2(\Delta z)^2}{\pi^2 n^2 w_0^4} \right)$$

$w_0$  = beam waist at focus,  $D_T$  = diffusion coefficient,  $\lambda$  = wavelength of light = 543 nm,  $n$  = refractive index of the medium = 1.33,  $z$  = axial distance,  $G(\tau)$  = auto correlation function

## 1.6. Line-Confocal Raman Spectroscopy- Instrumentation and Data Analysis

Raman spectra were obtained with a home-built line-confocal Raman microscope as line-confocal excitation has ~ 11 times more signal-to-noise ratio compared to point-confocal and provides better sensitivity even at relatively low power leading to less photodamage of the biological samples.<sup>4</sup> The instrumental details are previously been described in.<sup>4</sup> Briefly, Raman spectra were recorded using 350 mW (at the back aperture of the objective lens) of a commercially sourced 532 nm laser beam (Verdi-V10, Coherent, USA). The laser was used for the line excitation to the bilayer sample where the line was created using a cylindrical lens, and focused by a 60× water objective (N.A. 1.2). The scattered light coming from the sample was collected by the same objective lens and separated by a 532 nm ultra-steep long-pass edge filter (LP0- 532RE-25, Semrock), and then, focused at the line slit of 300 μm of an imaging spectrometer (Horiba iHR320, Japan) and finally detected on the rectangular chip of the CCD camera (Synapse, Model No. 354308, Horiba, Japan). All the experiments were performed at room temperature. Each spectrum was acquired between 2650 and 3050  $\text{cm}^{-1}$  (ν(C-H) region) with an integration time of 4 s and a total acquisition time of 13 minutes. The Raman spectra of this region of the membrane contain information about the order of the membrane (67-70). Intensities of scattered light were measured in increments of 0.018 nm (~0.5  $\text{cm}^{-1}$ ). From each acquired bilayer Raman spectrum, first, the water Raman spectrum was subtracted. After obtaining the subtracted spectrum, a linear baseline was fitted between 2650 and 3050  $\text{cm}^{-1}$  and then subtracted to obtain the final spectrum. This spectrum was normalized to unity intensity at a 2885  $\text{cm}^{-1}$  peak. The band intensities at 2850, 2885 and 2930  $\text{cm}^{-1}$  were calculated as the maximum of the intensity nearest to the respective wavenumber. The spectra were smoothed using the Savitzky-Golay method (five data points, second-order polynomial). We have then measured the ratios of intensities  $I_{2885}/I_{2850}$  and  $I_{2850}/I_{2930}$  as these ratios are related to the order of the membrane. In general, the higher the value of the  $I_{2885}/I_{2850}$  ratio, the more is the coupling between the lipid chains and thus, the more ordered is the membrane. The higher the value of the  $I_{2850}/I_{2930}$  ratio, the lesser will be

the rotational freedom of the terminal methyl group in the lipid chains and thus, the more ordered is the membrane. We have measured the effect of serotonin on these two parameters of the model SLBs using Line-Confocal Raman spectroscopy. The serotonin is incubated for 45 minutes to obtain changes in the Raman peaks for all the experiments.

## 1.7. Steady-state anisotropy measurements

Steady-state fluorescence anisotropy measurements of DPH and TMA-DPH in membranes were carried out using Hitachi F-7000 (Japan) spectrofluorometer. Fluorescence anisotropy values were calculated using the following equation:

$$r = \frac{I_{VV} - GI_{VH}}{I_{VV} + 2GI_{VH}} \quad (6)$$

where  $G = I_{HV}/I_{HH}$ , (grating correction or G-factor),  $I_{VV}$  and  $I_{VH}$  are the measured fluorescence intensities with the excitation polarizer vertically oriented, and the emission polarizer vertically and horizontally oriented, respectively. Both TMA-DPH and DPH were excited at 360 nm and their corresponding emission was monitored at 430 nm.

## 1.8. $^2\text{H}$ NMR measurements

Lipids were dissolved in 1:1 MeOH: chloroform and serotonin were dissolved in MeOH and co-dissolved for the serotonin-containing samples. To obtain a dry sample, the solvents were evaporated in a rotary evaporator at a 40°C water bath. To acquire a fluffy powder, the samples were re-dissolved in cyclohexane and lyophilized overnight at a high vacuum. Subsequently, the samples were hydrated with 50%wt HEPES buffer (20 mM HEPES, 0.1 mM EGTA, 150 mM NaCl). 10 freeze-thaw cycles between liquid nitrogen and a 40°C water bath were performed to produce multilamellar vesicles. To provide an inert environment for measurements, the samples were then inserted into 4 mm NMR rotors.

$^2\text{H}$  NMR spectra were measured on a Bruker 750 Avance I NMR spectrometer at a resonance frequency of 115.1 MHz. A 5 mm double-channel solids probe was used. A phase-cycled quadrupolar echo sequence was used for signal acquisition<sup>5</sup> with a 30  $\mu\text{s}$  delay between two  $\pi/2$  pulses of 2.5-4  $\mu\text{s}$  length. The spectral width was 500 kHz. The temperature of 25°C was used for all measurements. All NMR parameters were calculated using programs written in Mathcad software, as previously described.<sup>6</sup> To calculate the order parameters, the  $^2\text{H}$  NMR spectrum was first dePaked to obtain smoothed order parameters as described in.<sup>7</sup> The NMR order parameter is obtained by one measurement. The standard deviation is assumed to be 3 times of the sensitivity of measurement (which is 0.001 unit).

## 2. Effect of serotonin on the ‘membrane order’ of model membrane

### 2.1. Serotonin induced perturbation of POPG membrane

The effect of serotonin on the POPG membrane is probed using AFM force indentation, Nile red spectral imaging and NMR order parameter.

**2.1.1. AFM force indentation-** We have measured the  $F_X$  of POPG SLB in the absence and presence of 5 mM serotonin using AFM force indentation. Figure S1A shows the representative histograms of  $F_X$  of POPG in the absence (black) and presence (red) of 5 mM serotonin. The histogram shows that  $F_X$  of the POPG bilayer increases in the presence of serotonin. The average  $F_X$  (% increase in force = [Average  $F_X$  of POPG bilayer in 5 mM serotonin - Average  $F_X$  of POPG bilayer in 0 mM serotonin] \* [100/ Average  $F_X$  of POPG bilayer in 0 mM serotonin]) increases by  $(368 \pm 158)$  % (Figure S1B), suggesting that POPG bilayer becomes more ordered in the presence of 5mM serotonin.

**2.1.2. Spectral imaging of Nile Red-** We have then measured the Nile red fluorescence spectra bound to POPG SLB in the absence (Figure S1C, black curve) and the presence of 5 mM serotonin (Figure S1C, red curve). The serotonin containing membranes has clearly blue-shifted fluorescence spectra compared to that without serotonin. The average G/R ratios in the absence and presence of serotonin are  $(0.34 \pm 0.04)$  to  $(0.66 \pm 0.05)$  respectively, showing an increase of  $(94 \pm 22)$  % in the average G/R value. This suggests that the POPG membrane becomes more ordered after 5mM serotonin addition.

**2.1.3. Solid-State NMR-** We have also measured the order parameter of the POPG vesicles in the absence and presence of 10 mol% serotonin using solid-state NMR (Figure S1D). The NMR measurement has shown that the order parameter of the POPG bilayer along the lipid acyl chain does not change in the presence of serotonin (Figure S1D and S1E), suggesting that the order of the POPG membrane is not altered by serotonin.

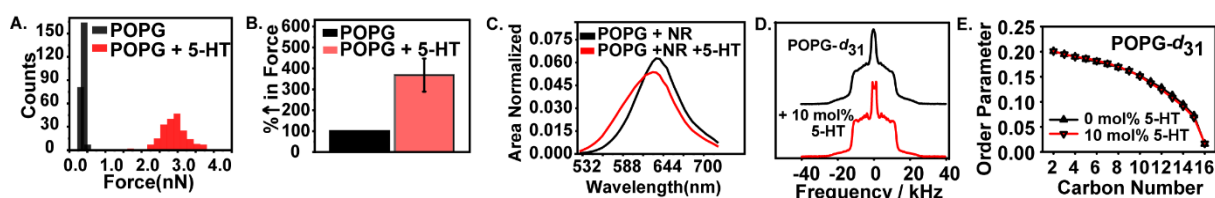


Figure S1. Effect of serotonin on the mechanical properties of POPG bilayer probed by different techniques. (A) A representative histogram of  $F_X$  on the POPG bilayer in the absence (black) and presence (red) of 5 mM serotonin. (B) Relative change in the average value of the  $F_X$  of POPG bilayer in the absence (black) and presence (red) of 5 mM serotonin (average of  $N = 4$  measurements). (C) The fluorescence spectra of membrane-bound Nile Red dye in the POPG bilayer in the absence (black) and presence (red) of 5 mM serotonin (average of  $N = 3$  measurements). (D)  $^2\text{H}$  NMR spectra of POPG- $d_{31}$  in the absence and presence of 10 mol% serotonin. (E) The  $^2\text{H}$  NMR order parameter along the deuterated lipid chains for POPG-  $d_{31}$  in the absence and presence of 10 mol% serotonin. Error bar is S.E.M. All experiments are carried out in the buffer.

## 2.2. Serotonin induced perturbation of phase-separated DEC221 membrane

Here, we probed the effect of serotonin on the biphasic model membrane DEC221 using AFM force indentation, Nile red, Laurdan and FCS techniques.



**2.2.1. AFM force indentation-** DEC221 at room temperature phase separates to form ordered and disordered phases. The phases are visualized by AFM imaging.<sup>8</sup> In our previous study<sup>8</sup>, we have measured the  $F_X$  of ordered and disordered phases separately in the absence and presence of 5 mM serotonin using AFM force indentation. Figures S2A and S2B (reproduced from Dey et al.<sup>8</sup>) show the representative histograms of  $F_X$  of disordered and ordered phases of DEC221 in the absence (black) and presence (red) of 5 mM serotonin. The histograms show that  $F_X$  of both the phases of the DEC221 bilayer decrease in the presence of serotonin. The average  $F_X$  are quantified for both the phases in the absence and presence of serotonin in Figure S2C (reproduced from Dey et al.<sup>8</sup>). The average  $F_X$  of the ordered phase is higher than the disordered phase by  $\sim 92\%$ . This clearly says that ordered phases are stiffer than disordered phases. The average  $F_X$  decrease both in the ordered as well as disordered phases in the presence of 5 mM serotonin (Figure S2A and S2B) by  $(52.0 \pm 8.3)\%$  and  $(32.0 \pm 10.3)\%$  respectively (Figure S2C), suggesting that serotonin makes both the membrane phases more disordered.

**2.2.2. Spectral imaging of Nile Red-** We have measured the serotonin-induced change in the fluorescence spectra of Nile red bound to DEC221 bilayer separately in ordered and disordered phases. We find that Nile Red has a preference for the disordered phase compared to the ordered phase by doing simultaneous AFM-confocal imaging of DEC221 incubated with Nile red. In this case, membrane phases are probed by AFM (Figure S2D) and fluorescence of Nile red is probed by confocal (Figure S2E) simultaneously by a home built combined AFM-confocal set-up (setup explained in our published work<sup>3</sup>), and by combining both the AFM and confocal images, phase-specific binding of Nile red is determined. We find that Nile red dye has  $\sim 4$  times more binding in the disordered phase compared to the ordered phase. This preference resulted in the intensity contrast in the fluorescence confocal image. Because of this contrast, we are able to extract fluorescence spectra specific to ordered and disordered phases separately from the spectral image. The fluorescence spectra of Nile red in the disordered and ordered phases in the absence (Figure S2F and S2G, black curves) and the presence of 5 mM serotonin (Figure S2F and S2G, red curves) are shown respectively. The spectrum of Nile red in the ordered phase has more contribution of lower wavelength compared to the disordered phase and fluorescence peak in the ordered phase is  $\sim 8$  nm shifted to lower wavelength compared to disordered phase (Figure S2F and S2G, black curves). This suggests that the ordered phase in fact is more ordered compared to the disordered phase. The serotonin containing membrane has a  $\sim 5$  nm shift towards a lower wavelength with G/R increases from  $(0.78 \pm 0.01)$  to  $(0.85 \pm 0.05)$  for the ordered phase (average G/R value increases by  $(9 \pm 6)\%$ ). There is no significant shift in the peak maxima of Nile red spectra in the presence of serotonin for the disordered phases. The G/R value increases from  $(0.52 \pm 0.01)$  to  $(0.59 \pm 0.02)$  by serotonin (average G/R value increases by  $(13 \pm 4)\%$ ). This suggests that both the phases become more ordered after 5 mM serotonin addition.

**2.2.3. Spectral imaging of Laurdan-** The multiphoton imaging of the Laurdan dye bound to the DEC221 bilayer is performed. The average GP value of the disordered and ordered phases of DEC221 bilayer in the absence (Figure S2H and S2I, black bars) and presence (Figure S2H and S2I, red bars) of 5 mM serotonin is calculated respectively. We find that the GP value of ordered phases is higher than the disordered phases (S2H, S2I, black bars). This suggests that the ordered phases are indeed more ordered than the disordered phases. We further find that the Laurdan GP value increases from  $(-0.16 \pm 0.01)$  to  $(-0.06 \pm 0.01)$  in the disordered phase and from  $(0.30 \pm 0.05)$  to  $(0.42 \pm 0.06)$  in the ordered phase. The average

GP value increases by  $(40 \pm 27) \%$  (Figure S2I) and  $(63 \pm 10) \%$  (Figure S2H) in the ordered and disordered phases respectively. The increase in GP indicates that both the phases in DEC221 become more ordered in the presence of serotonin.

**2.2.4. Z-FCS measurements-** We have also looked at how the diffusion properties of lipids in the DEC221 bilayer are changed by serotonin. We have measured the diffusion coefficients of 0.5 mol% Liss Rhod PE doped DEC221 by z-FCS. At given xy coordinates on the bilayer, we have measured the autocorrelation functions at different axial z distances and fitted each autocorrelation function using equation 2 to get characteristic diffusion times of lipids. The obtained diffusion times at different z-interval for the DEC221 bilayer in the absence (Figure S2J, scatter black square points) and presence of 5 mM serotonin (Figure S2K, scatter black square points) are fitted by equation 5 to obtain the diffusion coefficient value of lipids in the DEC221 bilayer in the absence (Figure S2J, red curve) and presence of serotonin (Figure S2K, red curve). The average diffusion coefficients of DEC221 bilayer in the absence (Figure S2L, black bar) and the presence (Figure S2L, red bar) of serotonin are  $(5.4 \pm 0.5)$  and  $(1.6 \pm 0.1) \mu\text{m}^2\text{s}^{-1}$ . The  $D_T$  of the DEC221 bilayer decreases by  $(70 \pm 11) \%$ , suggesting that the DEC221 bilayer becomes more ordered in the presence of serotonin.

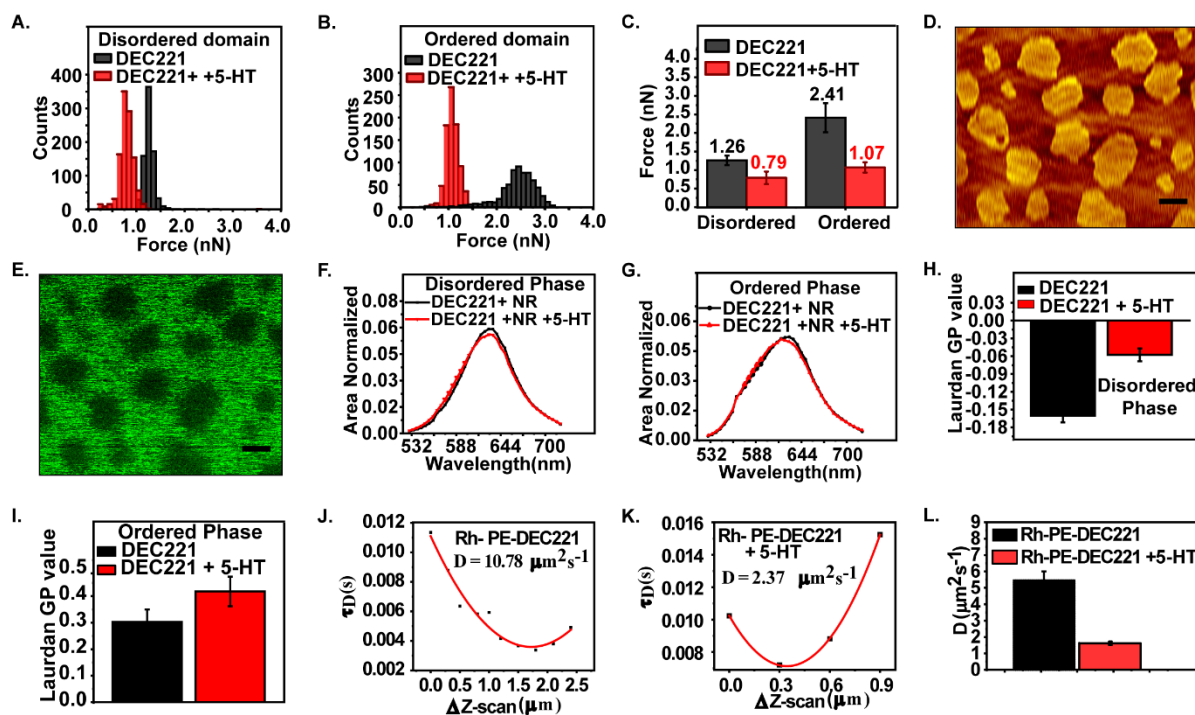


Figure S2. Effect of serotonin on the membrane properties of biphasic DEC221 bilayer. (A and B) The representative histograms of BFs on the disordered and ordered phases of DEC221 bilayer in the absence (black) and presence (red) of 5 mM serotonin (reproduced from Dey et al.<sup>25</sup>). (C) Average  $F_X$  of DEC221 bilayer in the disordered and ordered phases in the absence (black) and presence (red) of serotonin (reproduced from Dey et al.<sup>25</sup>). The numbers shown on each bar are the average  $F_X$  value. (D and E) A representative AFM and confocal images of DEC221 SLB incubated with  $\sim 100$  nM Nile Red. Scale bar =  $1\mu\text{m}$ . (F-G) The fluorescence spectra of membrane-bound Nile Red dye in the disordered (F) and ordered (G) phases of DEC221 bilayer in the absence (black) and presence (red) of 5mM serotonin (average of  $N = 3$  measurements). (H-I) GP value of Laurdan dye in the disordered (H) and ordered (I) phases of DEC221 bilayer in the absence (black) and presence (red) of 5mM

serotonin (average of  $N = 4$  measurements). (J-K) Probing diffusion coefficient of DEC221 bilayer containing 0.5 mol% Liss Rhod PE by z-FCS. Representative scatter plots of diffusion times of Liss Rhod PE in the DEC221 bilayer in the absence (J) and presence (K) of 5mM serotonin at different  $z$  intervals (black square points) and fitted by equation 5 (red curve) to obtain the diffusion coefficient of DEC221 bilayer. (L)  $D_T$  of DEC221 bilayer in the absence (black) and presence (red) of 5mM serotonin (average of  $N = 2$  measurements). Error bar is S.E.M. All experiments are carried out in the water.

## References:

- (1) Leonenko, Z. V.; Carnini, A.; Cramb, D. T. Supported Planar Bilayer Formation by Vesicle Fusion: The Interaction of Phospholipid Vesicles with Surfaces and the Effect of Gramicidin on Bilayer Properties Using Atomic Force Microscopy. *Biochim. Biophys. Acta - Biomembr.* **2000**, *1509* (1–2), 131–147. [https://doi.org/10.1016/S0005-2736\(00\)00288-1](https://doi.org/10.1016/S0005-2736(00)00288-1).
- (2) Hutter, J. L.; Bechhoefer, J. Calibration of Atomic-force Microscope Tips. *Rev. Sci. Instrum.* **1998**, *64* (7), 1868. <https://doi.org/10.1063/1.1143970>.
- (3) Gupta, A.; Dey, S.; Bhowmik, D.; Maiti, S. Coexisting Ordered and Disordered Membrane Phases Have Distinct Modes of Interaction with Disease-Associated Oligomers. *J. Phys. Chem. B* **2022**, *126* (5), 1016–1023. <https://doi.org/10.1021/ACS.JPCB.1C09421>/ASSET/IMAGES/LARGE/JP1C09421\_0003.JPEG.
- (4) Kumar Maity, B.; Das, A.; Dutta, S.; Maiti, S. Design and Construction of a Line-Confocal Raman Microscope for Sensitive Molecules. <https://doi.org/10.1007/s40010-018-0517-3>.
- (5) Davis, J. H.; Jeffrey, K. R.; Bloom, M.; Valic, M. I.; Higgs, T. P. Quadrupolar Echo Deuteron Magnetic Resonance Spectroscopy in Ordered Hydrocarbon Chains. *Chem. Phys. Lett.* **1976**, *42* (2), 390–394. [https://doi.org/10.1016/0009-2614\(76\)80392-2](https://doi.org/10.1016/0009-2614(76)80392-2).
- (6) Huster, D.; Arnold, K.; Gawrisch, K. Influence of Docosahexaenoic Acid and Cholesterol on Lateral Lipid Organization in Phospholipid Mixtures. *Biochemistry* **1998**, *37* (49), 17299–17308. <https://doi.org/10.1021/bi980078g>.
- (7) Lafleur, M.; Fine, B.; Sternin, E.; Cullis, P. R.; Bloom, M. Smoothed Orientational Order Profile of Lipid Bilayers by <sup>2</sup>H-Nuclear Magnetic Resonance. *Biophys. J.* **1989**, *56* (5), 1037–1041. [https://doi.org/10.1016/S0006-3495\(89\)82749-3](https://doi.org/10.1016/S0006-3495(89)82749-3).
- (8) Dey, S.; Surendran, D.; Engberg, O.; Gupta, A.; Fanibunda, S. E.; Das, A.; Maity, B. K.; Dey, A.; Visvakarma, V.; Kallianpur, M.; Scheidt, H. A.; Walker, G.; Vaidya, V. A.; Huster, D.; Maiti, S. Altered Membrane Mechanics Provides a Receptor-Independent Pathway for Serotonin Action. *Chem. - A Eur. J.* **2021**, *27* (27), 7533–7541. <https://doi.org/10.1002/chem.202100328>.